Contents lists available at YTUEJS

Journal of Sustainable Construction Materials and Technologies

https://jscmt.org/

Research Article

Rubberized Mortar from Rubber Tire Waste with Controlled Particle Size

Diego David Pinzón Moreno[a], Sebastião Ribeiro[a], Clodoaldo Saron[a,*]

aDepartment of Materials Engineering, Engineering School of Lorena, University of São Paulo, LOM-EEL/USP, Polo Urbo Industrial, Gleba AI-6, s/n, CEP: 12602-810, Lorena, SP, Brazil

Abstract

The generation of new materials such as rubberized mortar presents itself as an alternative to the decrease environmental problems generated due to the inadequate management of scrap tires, reaching high economic potential and environmental sustainability. In this study, mortar composites were prepared from Portland blast-furnace slag cement (type IS) and rubber granular waste from unusable tires of different commercial-brands with the purpose of evaluating the effects of the rubber particle size and rubber content on mechanical, chemical and morphological properties of the composites. Rubberized mortar has shown considerable improvement in flexural strength, strain and apparent density when compared to the conventional mortar, while the size particle of the rubber caused insignificant changes on these properties. Thus, rubberized mortar shows promising potential for the use of the material in applications where flexural strength is essential.

Keywords: Mortar; Rubber; Tire; Recycling; Particle Size; Composites

1. Introduction

The inappropriate disposal of scrap tires causes serious environmental problems worldwide [1,2]. The global tire manufacturing output was estimated at over 17 million tonnes in 2016 with providing an annual growing nearly at 4% through 2022 [3]; these tires will eventually become solid waste with pollutant potential [4].

On the other hand, some alternatives have been employed to minimize the problem such as reuse of tires by retreading, burning for energy recovery, recycling and application as ground rubber products, recycling by devulcanization methods and pyrolysis for generation of several products [1-6]. Thus, the greater number of alternatives for consuming of scrap tires contributes to a decrease the amount in tires waste in the environment. In this sense, the incorporation of tire rubber particles in materials widely used in the world such as asphalt and mortar is very interesting. Moreover, news materials with modified properties can be generated for specific applications [7].

Studies on the development of mortar or concrete composites with rubber aggregates of different sizes, morphologies and treatments have been performed, causing interest in different commercial and academic sectors [8-13]. Naturally, the use of polymeric aggregates in cement matrix generates challenges on the material due to the difficulty in obtaining interface adhesion between phases of different chemical characteristics. In the production of mortars and concretes, the pozzolanic activity of the cement plays a fundamental role in the final properties. However, there is not a chemical reaction between the rubber aggregates and the cement, preventing the improvement of properties in the generation of mortars and concretes rubberized [11, 14-17]. Therefore, the content rubber, as well as the particle size of the rubber, incorporate in the mortar can result in considerable variation in the performance of the material properties. Thus, the aims of this present study have been to evaluate the effects of

low rubber content and of the rubber particle sizes on the properties of rubberized mortar prepared with commercial Portland cement and recycled rubber from scrap tires.

2. Experimental

2.1. Materials

For rubberized mortar preparation, it was used commercial Portland blast-furnace slag cement (type IS), according to the ASTM C595[18], manufactured by the Companhia Siderúrgica Nacional (CSN), sand as an aggregate of natural source from the Paraíba do Sul river basin, which is classified as medium and pre-washed, and rubber waste obtained from the tire retreading process when the tire covering is partially scraped and cut by means of a process with rotary knives, generating a rubber waste in elongated granular form. The tires are from different brands, leading to an unspecified composition of the rubber waste.

2.2. Materials preparation

Before preparation of the composites, the sand was sieved to remove impurities and to define the particle size distribution, which was verified between 150 to 600 μm, ensuring the homogeneity and reproducibility of the samples. On the other hand, before mixing the mortar, the moisture content in the sand was evaluated in order to correct the water trace in the case of having considerable water contents in the aggregate, trying to maintain the proportions of the constituents of the mortar without variation at the mixing time. Additionally, the rubber waste was sieved to the separation of different particle sizes.

The mortar preparation was performed in a mechanical mixer, Metal Cairo AG-5: 2008, with spindle rotation and planetary movement. Firstly the water was added to the vat, which was followed by cement, sand and rubber, respectively. All conditions for mortar blending were based on ASTM C305 standard [19].

Specimens were prepared for axial compressive and flexural tests. Thus, seven compositions for flexural test and seven other compositions for the axial compressive test were prepared, in addition to the reference compositions for each type of test. Three granulometric ranges of rubber were used for each composition. Table 1 describes the samples identification based on the content and particle size of the rubber in the different compositions. Table 2 shows the ratio of components used in the preparation of the mortar for all the compositions, following recommendations of the standard practice ASTM C305 [19].

Table 1. Samples identification

Rubber Content (wt%)	Fine particle size rubber (0.85 to 1.68 mm)	Medium particle size rubber (1.68 to 2.38 mm)	Coarse particle size rubber (2.38 to 3.38 mm)
0	R	R	R
1	S1	M1	L1
2	S2	M2	L2
3	S3	M3	L3
4	S4	M4	L4
6	S6	M6	L6
8	S8	M8	L8
10	S10	M10	L10

Table 2. Mortar components

Component	Proportion by weight (kg)	Percentage (wt%)
Cement	1,00	23,64
Sand	2,75	65,01
Water	0,48	11,35

All compressive and flexural sample molds were sealed with adhesive and tape to ensure tightness. At the same time, all the molds were covered with a light coat of oil to ensure the proper demolding of the specimens. Immediately, the material was placed in the molds in the shortest possible time, after mixing. For each sample, the material was placed in three layers receiving each layer 30 uniform strokes with an ordinary socket. This molding is completed by placing each of the samples on an automatic vibrator Sieve agitator at 3600 vibrations/min (vpm) for 1 minute. After molding, the material was pre-cured and cured in according to standard practice ASTM C109 [20]. For the development of the mechanical tests, the specimen's surface was firstly ground and polished in horizontal grinding Ferdimat machine T42:2005-600 mm.

2.3. Characterization

Axial compressive and flexural tests, scanning electron microscopy (SEM), X-ray fluorescence (XRF), surface area analysis (BET), and apparent density (AD) were performed for characterization of mechanical, chemical and morphological properties of the material.

Axial compressive and flexural tests were performed in a universal electromechanical test machine (maximum load of 100 kN) EMIC-DL10000/700 at a speed of 0.5 mm/min, using four specimens for each mix design, according to the recommendations of the standard practice ASTM C109 [20].

For the flexural test, the three-point flexural strength (S_f) was calculated by equation 1, according to the recommendations of the standard practice ASTM C348 [21].

$$S_f = 3PL/2bh^2 \tag{1}$$

Where P is the maximum force that supports each test specimen, L and the distance between supports, *b* is the length of the base of the specimen and h is the height of the specimen. The average compressive strength (S_f) was obtained by the numerical average of the four specimens previously tested.

SEM micrographs were obtained in a HITACHI TM3000 equipment, employing secondary electron signal and voltage of 20 kV. The samples for SEM micrographs were removed from fracture surface of the specimens for mechanical testing and placed on a steel plate by gluing a carbon tape and applying a thin gold layer of approximately 20 nm in a MED020 metallizer (BAL-TEC/MCS MULTICONTROL SYSTEM). In addition, a carbon tape was also placed on the sides of the samples, from the base to the sample surface, to electrically ground the fracture surface.

X-ray fluorescence (XRF) was performed in a Panalytical X-ray fluorescence spectrometer, model AXIOS.

Specific area analysis (SAA) using the Brunauer-Emmett-Teller (BET) method was carried out in a triStar II Instrument Plus Micromeritics Instrument. For the analysis, the rubber samples were subjected at 110 °C for 2 hours for degasification, while for sand and cement was used degassing at 200 °C for 2 hours. On the other hand, the apparent density (AD) was obtained based on the methodology of the standard practice ASTM C642 [22] by the arithmetic mean of the samples (triplicate).

3. Results and discussion

3.1. Chemical and morphological analysis of the raw materials

The results obtained by the XRF analysis of the chemical composition of the cement, rubber, and sand are presented in Table

Table 3. Chemical composition of Portland cement, rubber and sand.

| Chemical component (wt%)	Portland Cement	Rubber	Sand
CaO	54.79	0.21	0.29
SiO_2	24.72	1.95	89.6
Al_2O_3	7.78	0.2	5.96
MgO	4.95	0.16	0.44
SO_3	2.89	0.18	--
Fe_2O_3	2.5	0.15	0.59
K_2O	0.64	0.04	2.07
Na_2O	0.33	--	0.73
MnO	0.56	--	--
TiO	0.5	--	0.17
P_2O_5	--	0.06	0.04
Cl	--	0.01	0.02
ZnO	--	1.53	0.03
SrO	0.18	--	--
OF*	--	95.49	--

(*) Organic and sulfur fraction.

The chemical composition experimentally obtained for cement by XRF is in accordance with the established values by the Brazilian standard NBR 5735 states, determinating that the composition of the cement type IS may vary depending on the chemical composition of the raw materials used and mainly on the basis of revenue, since the standard allows ranges with varying raw material dosages.

XRF analysis of the rubber waste has been performed after calcination of the material. This procedure is necessary to eliminate the organic and sulfur fraction of the material for the analysis of the other inorganic components. It can be noted that the organic and sulfur fraction of the rubber is approximately 95.49%, while the content of zinc oxide is also relatively high when compared to other oxides present in the material. Zinc is often incorporated to the rubber as zinc stearate with the purpose of leading to the

formation of surface layers on the rubber, which prevents the adhesion of the rubber with other substrates [14-17]. In the chemical analysis by XRF of the sand showed an approximate content of 90% for SiO_2, as the main constituent, and 6% for Al_2O_3, as the second major constituent.

Figure 1 shows the SEM micrographs of the cement. It is observed that the cement particles are in dimensions smaller than 25 μm and have several morphologies in which predominate smooth surfaces with sharp edges.
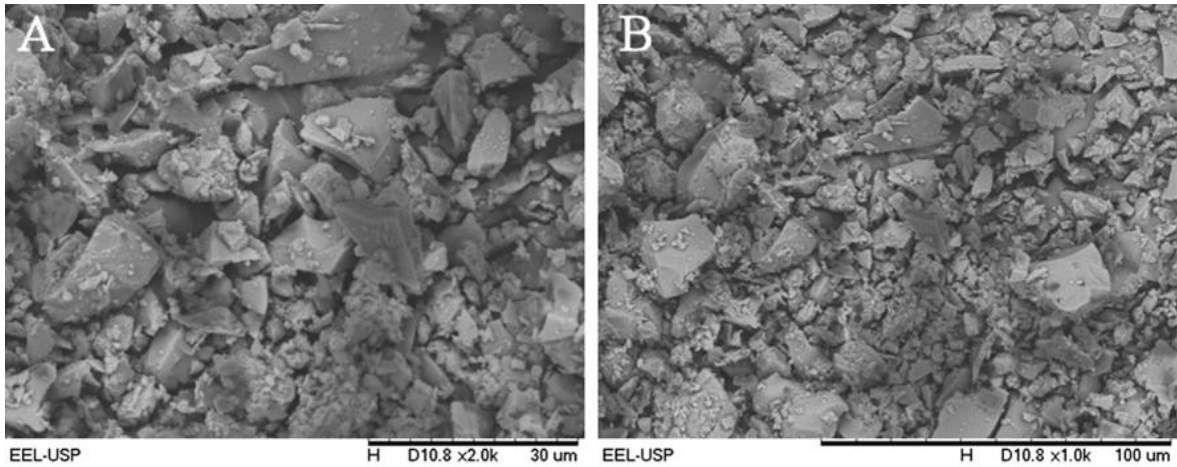
Figure 1. SEM micrograph of Portland cement: (a) 2.0 kx; (b) 1.0 kx.

The grain size ranges of the rubber waste were classified into three groups (Table 1) as coarse particles that pass through the sieve of 6-8 mesh (3.38 to 2.38 mm), medium particles of 8-10 mesh (2.38 to1.68 mm) and fine particles of 10-20 mesh (1.68 to 0.85 mm). The rubber particle size ranges were chosen based on the characteristic aggregate size used in a traditional mortar [23]. Figure 2 shows the SEM micrographs of the rubber with fine size on the range of 0.85 to 1.68 mm.
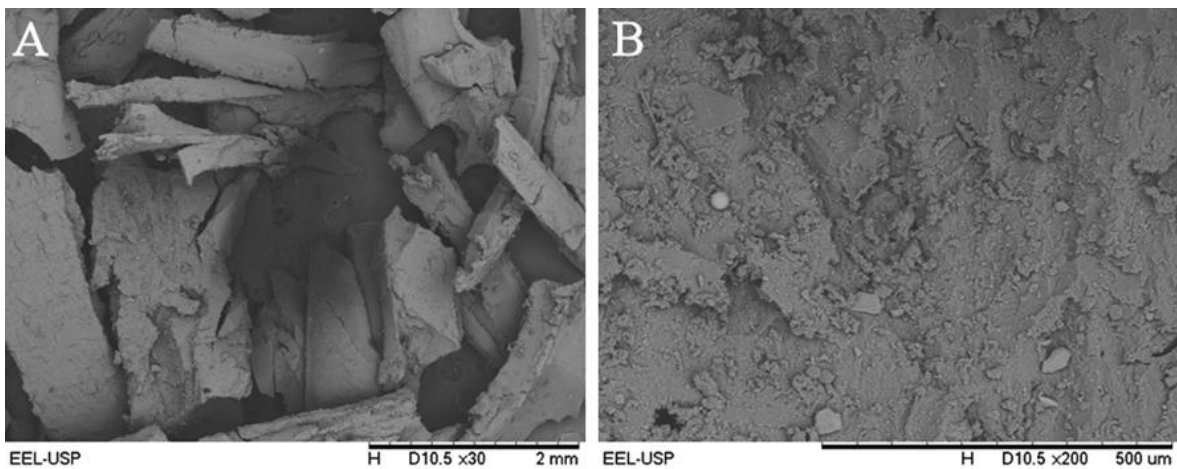
Figure 2. SEM micrograph of rubber: (a) 30x; (b) 200x.

The rubber particles present elongated shape and variable roughness due to the process of obtaining the rubber particles by scraping the tires. Additionally, it is observed that the samples have sharp edges. Table 4 presents the granulometry range of the sand which was determined by sieving.

Table 4. Sand granulometry

Particle size (μm)	Sand (wt%)
>600	Discarded
425	4%
300	66%
150	24%
<150	4%

It is observed five granulometric bands on the range of 150 to 600 μm, whose fraction with 300 μm is predominant. Particles larger than 600 μm have been discarded, while the other fractions were mixed for use as aggregate in the mortar. Specific surface area analysis (SAA) using the Brunaure-Emmett-Teller (BET) method shows for the sand a surface area of 0.18 m²/g, a pore

volume of 5.83 x 10^{-4} cm³/g and a pore size of 129.38 Å. For cement, the surface area is 1.06 m²/g, the pore volume is 3.88 x 10^{-3} cm³/g and the pore size is 146.74 Å. Cement has a larger surface area than sand due to the smaller particle size, while pore volume and pore size may be related to the particle roughness. For rubber, only the particle size ranges of 1.68 to 2.38 and of 2.38 to 3.38 mm showed results of 0.18 and 0.03 m²/g for surface area, respectively. Thus, smaller particles present a larger surface area and consequent high contact surface with mortar matrix in the rubberized mortar.

3.2. Mechanical properties of the rubberized mortar

Figure 3 shows representative stress-strain curves for rubberized mortar generated by compressive tests as a function of the content and particle sizes of the rubber. Both stress and strain decrease with increasing content of rubber waste in the mortar. Thus, the incorporation of the rubber to the mortar causes notable changes in the material properties. It can be better noted through results of compressive strength and maximum compressive deformation.
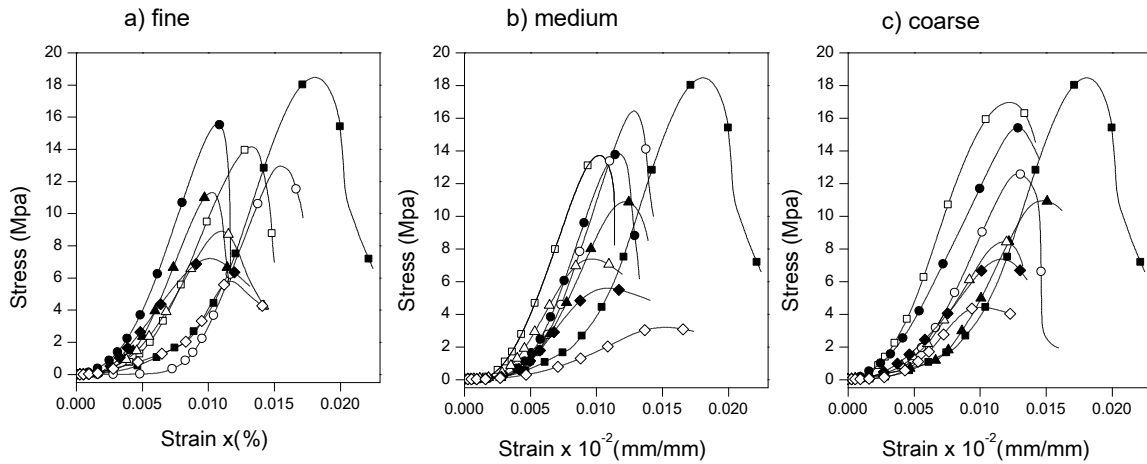
Figure 3. Stress-strain curves of compressive tests for rubberized mortar with different rubber sizes and rubber content. Rubber size: a) fine; b) medium and c) coarse. Rubber content: reference without rubber (■); 1 wt% (□); 2 wt% (●); 3 wt% (○); 4 wt% (▲); 6 wt% (Δ); 8 wt% (•) and 10 wt% (◊)

The results of the compressive strength are shown in Figure 4. Rubberized mortar shows a gradual decrease in the compressive strength with increasing rubber content in the material. This decrease in compressive strength has already been widely reported by several authors [24-27]. On the other hand, there is not a significant difference in the results of the compressive strength for the three different granulometries, showing that compressive strength does not depend on the rubber granulometry.
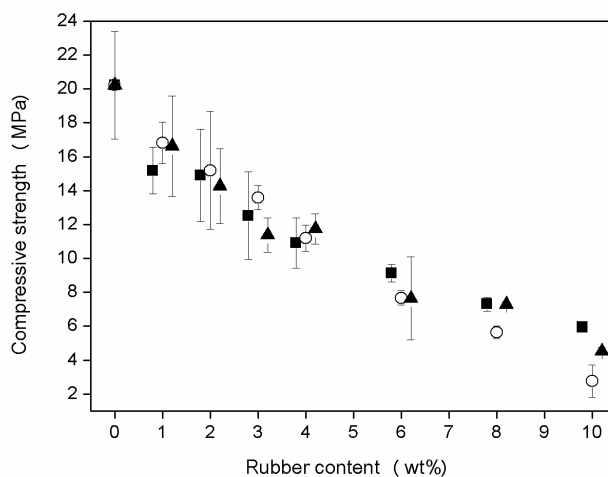
Figure 4. Compressive strength for rubberized mortar with: fine rubber particle (■); medium rubber particle (○) and coarse rubber particle (▲)

Figure 5 shows the deformation at fracture by the compressive test of the rubberized mortar. A deformation on the range of 0.9 to 2.1 mm is noted for all types of composites with different contents and granulometry of rubber. Therefore, the deformation at fracture does not depend on the presence of rubber in the mortar. The decrease in the compressive strength and the invariable compressive deformation with increasing content of the rubber in the composites can be caused because the particles of elongated

morphology generate insufficient adhesion forces in the material under compressive tensions to alter positively the compressive strength.
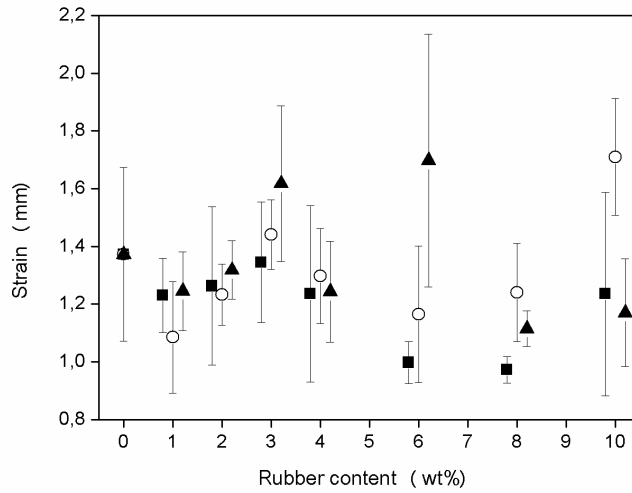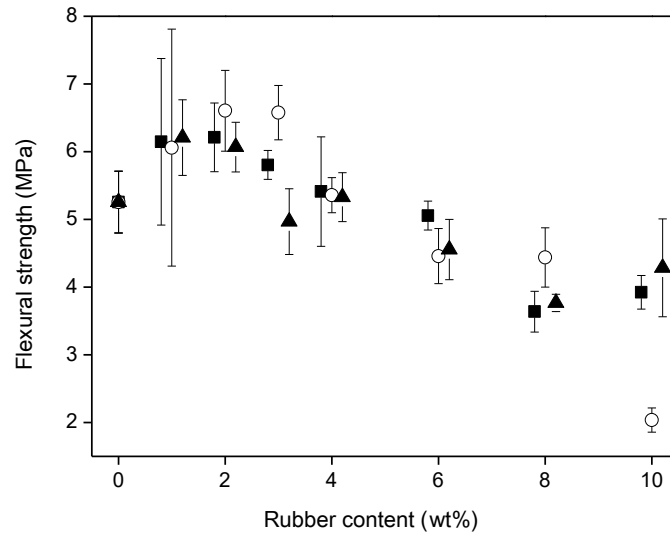

Figure 5. Maximum compressive deformation for rubberized mortar with: fine rubber particle (■); medium rubber particle (○) and coarse rubber particle (▲)

Figure 6 shows representative stress-deflection curves for rubberized mortar generated by flexural tests as a function of the content and particle size of the rubber. The mortars containing rubber at 0 to 4 wt% present the highest values of stress. However, the curves profiles change with increasing rubber content in the material. The behavior of the flexural strength of the rubberized mortar with different rubber contents is presented in Figure 7. The most important feature of the results is the preservation or increase of the flexural properties up to rubber content at around 4 wt%. At higher rubber contents, the flexural strength of the material decreases gradually. This is a plausible result since the required stress for rubber deformation is low when compared to others materials. Thus, the contribution of the rubber on the decrease in flexural strength is more significant as its content increases in the mortar. In parallel, like to the compressive test (Figure 4), it can be observed that the flexural strength is not affected by variation of the rubber granulometry indicating that in these grain sizes there is a similar mechanical property generated by them. On the other hand, it is important to note that despite the like behavior of the compressive and flexural strength of the mortar as a function of the rubber content, the absolute values for these properties are different, which corresponds to the differences in the behavior of the mortar under conditions of tension and compressive.
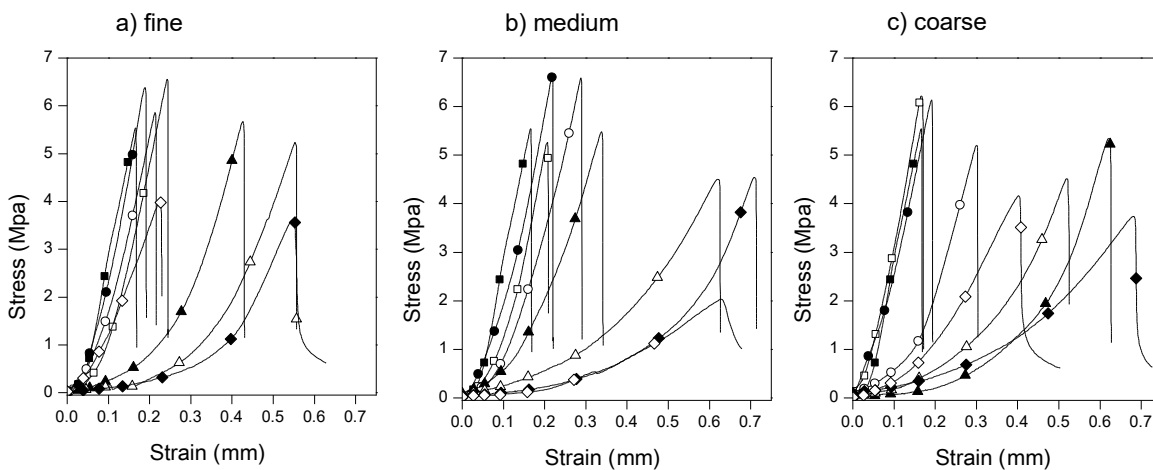

Figure 6. Stress-strain curves of flexural tests for rubberized mortar with different rubber sizes and rubber content. Rubber size: a) fine; b) medium and c) coarse. Rubber content: reference without rubber (■); 1 wt% (□); 2 wt% (●); 3 wt% (○); 4 wt% (▲); 6 wt% (Δ); 8 wt% (•) and 10 wt% (◊)

Figure 7. Flexural tensile strength for rubberized mortar with: fine rubber particle (■); medium rubber particle (○) and coarse rubber particle (▲)

Figure 8 presents the deflection generated in the flexural tests of the different compositions. It is observed that rubber contents lower than 4 wt% lead to the mortar with smaller deformations when compared to the mortar reference without rubber. However, at rubber contents higher than 4 wt% the deformations increase in relation to the reference composition. Thus, the deformations in the flexural test occur on range from about 0.15 to 0.9 mm. Additionally, an inverse behavior is observed when comparing the strength and the strain in the flexural test. Both curves present a sinusoidal behavior as a function of rubber content in the mortar. Thus, while the strength decreases for higher rubber contents, the strain proportionally increases for these values. On the other hand, this effect is inverse for lower rubber contents. The flexural resistance preservation up to around 5 wt% is possibly due to the elongated morphology particle that generates sufficient cohesive forces under tensile stresses to positively alter the flexural strength [24-27]. This feature allows advantageously selecting a processing radius depending on the requirements of the project where the material is to be employed.
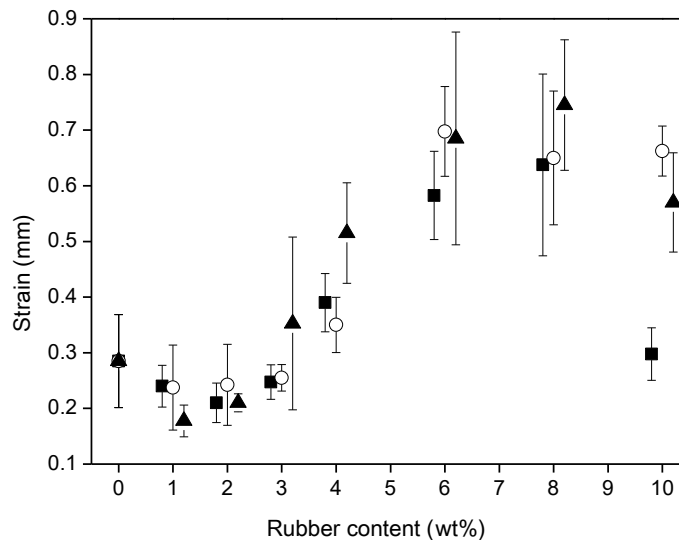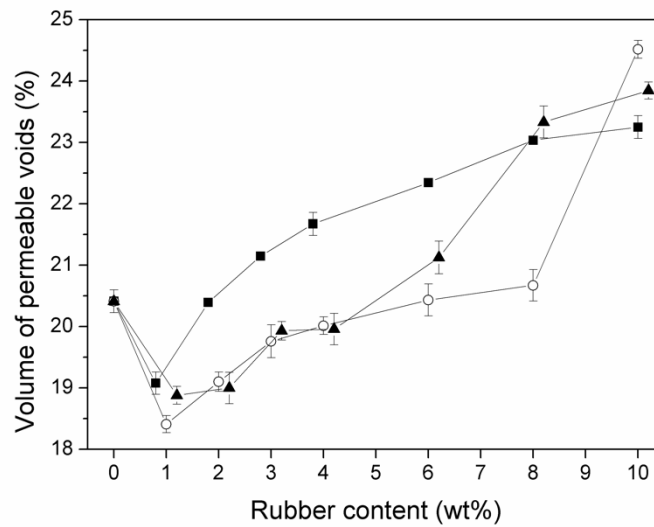

Figure 8. Maximum flexural deformation for rubberized mortar with: fine rubber particle (■); medium rubber particle (○) and coarse rubber particle (▲)

Figs. 9 and 10 show the apparent density and the volume of permeable voids, respectively. The apparent density curves show a clear decrease with the gradual increase of the rubber content independent of the kind of granulometry employed. However, when the rubberized mortars containing the same rubber content are compared, the apparent density is lower for the material prepared with the rubber of medium granulometry. For all compositions, the apparent density is in the range of 2.50 and 2.20 g/cm^3. It is important to highlight the relationship between the apparent density and the mechanical properties, where a decrease

of the properties is expected with the decrease of the density of the mortar composites. In addition, the decrease in apparent density is expected considering that the density of the rubber is much lower than the density of the mortar, consequently, the gradual replacement of the mortar by the rubber will generate a gradual decrease of the apparent density.
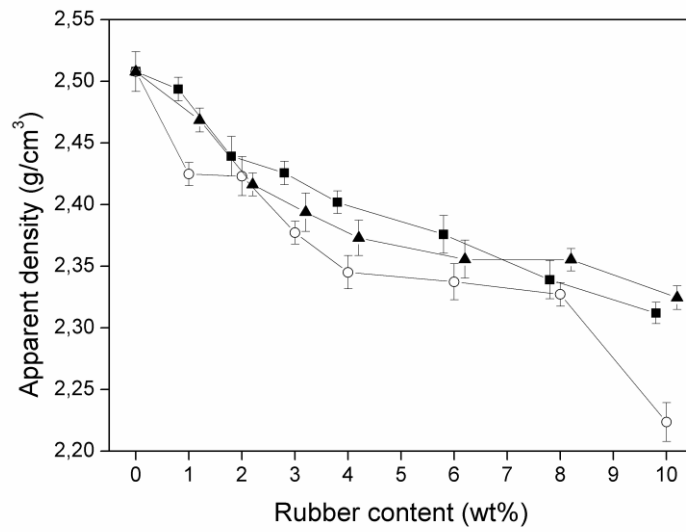
Figure 9. Apparent density for rubberized mortar with: fine rubber particle (■); medium rubber particle (○) and coarse rubber particle (▲).


Figure 10. Volume of permeable voids for rubberized mortar with: fine rubber particle (■); medium rubber particle (○) and coarse rubber particle (▲)

On the other hand, the percentage of the volume of the interconnected voids shows an increase with the growth of the content of the rubber aggregate. The organic character of the rubber, as well as the presence of zinc stearate on the rubber surface, should cause poor adhesion between the mortar and the polymer. This poor adhesion allows the localization of air at the interface between the mortar and the rubber [11]. Consequently, the volumetric fraction of permeable air voids increases with increasing surface area of the gradually increasing rubber aggregate in the mortar composite. This can justify the increase in the volume of permeable voids and the falls in the mechanical properties of most composites. Likewise, the result of the percentage of the volume of permeable voids was confirmed using the two methods explained in ASTM C642 [22].

Figure 11 shows representative SEM micrographs of the mortar with rubber aggregate. It was possible to identify the hydrated phases as portlandite, katoite, hydrated calcium silicate, and ettringite. These hydrated phases are the main responsible of the hardening and consequently of the increase in the different types of mechanical resistances. Additionally, other phases such as aggregates of cristobalite, quartz, gypsum, and lime-free are also observed. The presence of cristobalite and quartz are usually associated with non-reactive silica from the fine aggregate fraction of the mortar. In Figure 11a of the control sample without the addition of rubber can be distinguished the different phases of the mortar, observing the fine aggregate (sand) and cementitious matrix. Figure 11b shows the micrograph obtained by SEM of the sample with 2 wt% of rubber aggregate, where

is possible to distinguish the cement phase, fine aggregate (sand) and rubber aggregate in low proportion. On the other hand, Figure 11c shows the SEM micrograph of the composite containing 10 wt% rubber. In this case, morphological characteristics similar to the composition with 2 wt% of rubber are observed.
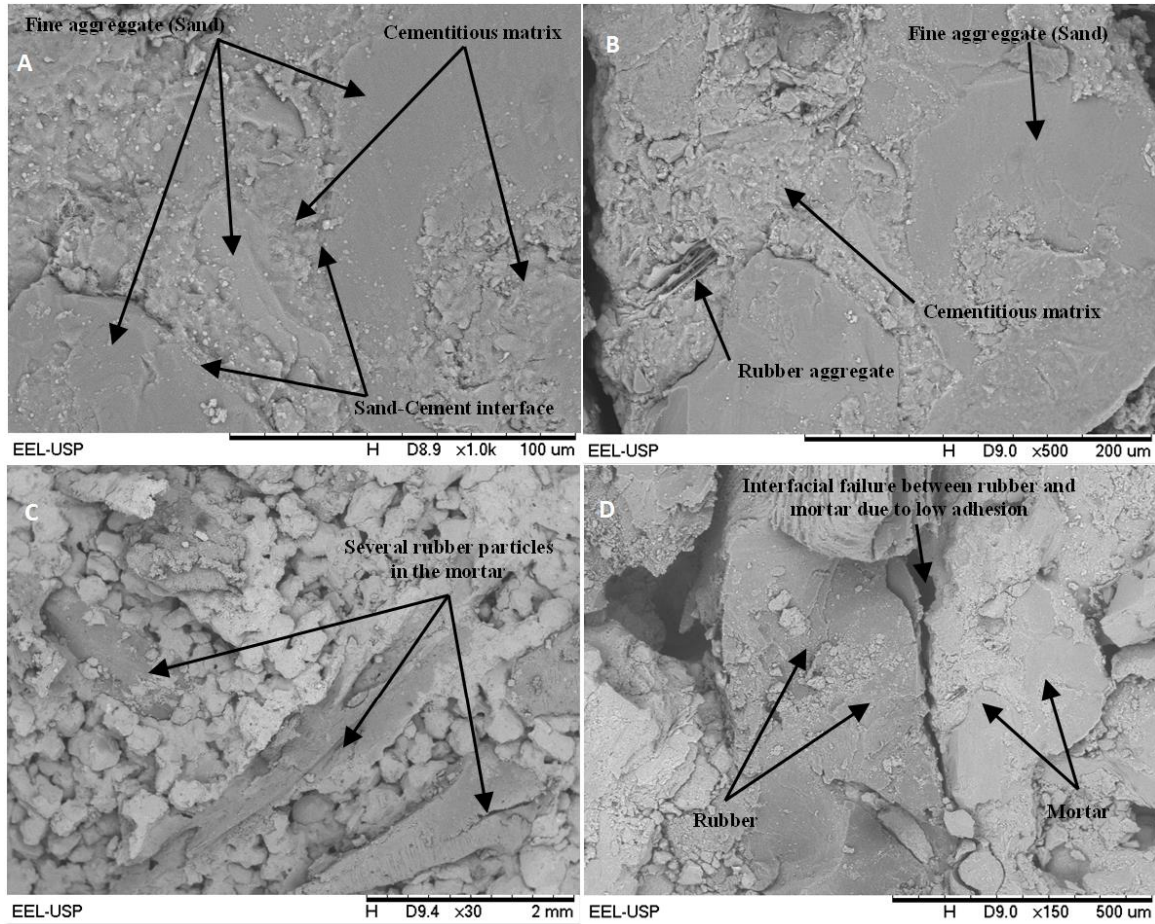
Figure 11. SEM micrograph of mortar: a) un-rubberized mortar; b) containing rubber at 2 wt%; c) containing rubber at 10 wt% and d) interfacial failure in rubberized mortar

The morphological distinction between the dispersed polymer phase and the ceramic matrix was based on the typical failure characteristics of both materials. The polymer fraction presents a high degree of deformation on torn shapes that in the case of the studied material may have this morphological attribute due to pre-treatments prior to processing or have obtained this characteristic during the treatments and/or mechanical tests of this project. On the other hand, the morphological characteristic of the surface of the mortar failure is the rough surface of the cementitious fraction or totally smooth of the fracture of the aggregate. Thus, it is possible to see in the mortar regions with pores. Likewise, energy-dispersive X-ray spectroscopy (EDS) analysis was used to distinguish the compositions of the polymer-ceramic phases of the composites.

Figure 11d shows the SEM micrograph of the mortar containing rubber at 10 wt%, focusing on the region of interfacial failure between the rubber aggregate and the mortar. Poor adhesion and void spaces can be visualized by the displacement of the rubber in the mortar. This displacement probably induces the propagation of cracks, triggering the catastrophic failure of the material. Moreover, the probability of presenting these types of faults increases by the presence of interfacial air between the mortar and the rubber aggregate and, accordingly, with the increase of the rubber content in the mortar, which justifies the decrease in the mechanical properties.

4. Conclusion

The presence of rubber particles as aggregate in mortar leads to the changes in mechanical properties of the material. Compressive strength progressively decreases as a function of the rubber content, while flexural strength increases when the rubber is incorporated to the mortar at low concentration. Flexural deformation also increases when the rubber content in the mortar is around 7 wt%. Thus, mechanical properties of the mortar are changed by inherent characteristics of the rubber, showing that there is interaction between rubber particles and ceramic matrix. However, the changes in rubberized mortar are strongly dependent of the rubber content in the mortar. On the other hand, the variation in the rubber particle size has shown insignificant changes on these properties. Rubber particle size affects properties as apparent density and volume of permeable voids, which

increase to rubberized mortar containing small rubber particles. The use of rubbers from tire waste in the mortar can be economically viable for applications where higher flexural strength is required. Thus, the production of rubberized mortar can be an interesting alternative for recycling of scrap tires.

Data Availability Statement
All graphs and data obtained or generated during the investigation appear in the published article.

Author's Contributions:
Diego David Pinzón Moreno: Assisted the experiment's progress and helped in manuscript preparation.
Sebastião Ribeiro: Assisted the experiment's progress and helped in manuscript preparation.
Clodoaldo Saron: Drafted and wrote the manuscript, performed the experiment and result analysis.

Conflict of interest
The authors declared no potential conflicts of interest with respect to the research, authorship, and/or publication of this article.

Ethics
There are no ethical issues with the publication of this manuscript.

References

[1] Czajczyńska, D., Krzyżyńska, R., Jouhara, H., & Spencer, N. (2017). Use of pyrolytic gas from waste tire as a fuel: A review. *Energy, 134*, 1121–1131. https://doi.org/10.1016/j.energy.2017.05.042

[2] Machin, E. B., Pedroso, D. T., & de Carvalho, J. A. (2017). Energetic valorization of waste tires. *Renewable and Sustainable Energy Reviews*, *68*, 306–315. https://doi.org/10.1016/j.rser.2016.09.110

[3] Rapra, S. (2018, June 06). The Future of Tire Manufacturing to 2022. https://www.smithersrapra.com/market-reports/tire-industry-market-reports/the-future-of-tire-manufacturing-to-2022

[4] Corredor-Bedoya, A., Zoppi, R., & Serpa, A. (2017). Composites of scrap tire rubber particles and adhesive mortar – Noise insulation potential. *Cement and Concrete Composites*, *82*, 45–66. https://doi.org/10.1016/j.cemconcomp.2017.05.007

[5] Al-Akhras, N. M., & Smadi, M. M. (2004). Properties of tire rubber ash mortar. *Cement and Concrete Composites*, *26*(7), 821–826. https://doi.org/10.1016/j.cemconcomp.2004.01.004

[6] Sienkiewicz, M., Kucinska-Lipka, J., Janik, H., & Balas, A. (2012). Progress in used tyres management in the European Union: A review. *Waste Management*, *32*(10), 1742–1751. https://doi.org/10.1016/j.wasman.2012.05.010

[7] Sodupe-Ortega, E., Fraile-Garcia, E., Ferreiro-Cabello, J., & Sanz-Garcia, A. (2016). Evaluation of crumb rubber as aggregate for automated manufacturing of rubberized long hollow blocks and bricks. *Construction and Building Materials*, *106*, 305–316. https://doi.org/10.1016/j.conbuildmat.2015.12.131

[8] Si, R., Guo, S., & Dai, Q. (2017). Durability performance of rubberized mortar and concrete with NaOH-Solution treated rubber particles. *Construction and Building Materials*, *153*, 496–505. https://doi.org/10.1016/j.conbuildmat.2017.07.085

[9] Si, R., Guo, S., & Dai, Q. (2017b). Durability performance of rubberized mortar and concrete with NaOH-Solution treated rubber particles. *Construction and Building Materials*, *153*, 496–505. https://doi.org/10.1016/j.conbuildmat.2017.07.085

[10] Shi, C., Li, Y., Zhang, J., Li, W., Chong, L., & Xie, Z. (2016). Performance enhancement of recycled concrete aggregate – A review. *Journal of Cleaner Production*, *112*, 466–472. https://doi.org/10.1016/j.jclepro.2015.08.057

[11] Guo, S., Dai, Q., Si, R., Sun, X., & Lu, C. (2017). Evaluation of properties and performance of rubber-modified concrete for recycling of waste scrap tire. *Journal of Cleaner Production*, *148*, 681–689. https://doi.org/10.1016/j.jclepro.2017.02.046

[12] Segre, N., Monteiro, P. J., & Sposito, G. (2002). Surface Characterization of Recycled Tire Rubber to Be Used in Cement Paste Matrix. *Journal of Colloid and Interface Science*, *248*(2), 521–523. https://doi.org/10.1006/jcis.2002.8217

[13] He, L., Ma, Y., Liu, Q., & Mu, Y. (2016). Surface modification of crumb rubber and its influence on the mechanical properties of rubber-cement concrete. *Construction and Building Materials*, *120*, 403–407. https://doi.org/10.1016/j.conbuildmat.2016.05.025

[14] Aziz, A., Farah, N. A., Sani, M. B., Azline, N., & Jaafar, M. S. (2017). A Comparative Study of the Behaviour of Treated and Untreated Tyre Crumb Mortar with Oil Palm Fruit Fibre Addition. *Pertanika Journal of Science & Technology*, *25*(1), 101-120.

[15] Toutanji, H. (1996). The use of rubber tire particles in concrete to replace mineral aggregates. *Cement and Concrete Composites*, *18*(2), 135–139. https://doi.org/10.1016/0958-9465(95)00010-0

[16] Ganjian, E., Khorami, M., & Maghsoudi, A. A. (2009). Scrap-tyre-rubber replacement for aggregate and filler in concrete. *Construction and Building Materials*, *23*(5), 1828–1836. https://doi.org/10.1016/j.conbuildmat.2008.09.020

[17] Khatib, Z. K., & Bayomy, F. M. (1999). Rubberized Portland Cement Concrete. *Journal of Materials in Civil Engineering*, *11*(3), 206–213. https://doi.org/10.1061/(asce)0899-1561(1999)11:3(206)

[18] Youssf, O., ElGawady, M. A., Mills, J. E., & Ma, X. (2014). An experimental investigation of crumb rubber concrete confined by fibre reinforced polymer tubes. *Construction and Building Materials*, *53*, 522–532. https://doi.org/10.1016/j.conbuildmat.2013.12.007

[19] ASTM C305-06. (2016). Standard practice for mechanical mixing of hydraulic cement pastes and mortars of plastic consistency. ASTM West Conshohocken, PA.

[20] ASTM C109/C109M - 20b. (2016). Standard test method for compressive strength of hydraulic cement mortars (using 2-in. or [50-mm] cube specimens). *Annual Book of ASTM Standards*, *4*.

[21] ASTM C348. (1998) Standard test method for flexural strength of hydraulic-cement mortars. West Conshohocken, PA.

[22] ASTM C642-06. (2008). Standard test method for density, absorption, and voids in hardened concrete. West Conshohocken, PA.

[23] Benakli, S., Bouafia, Y., Oudjene, M., Boissière, R., & Khelil, A. (2018). A simplified and fast computational finite element model for the nonlinear load-displacement behaviour of reinforced concrete structures. *Composite Structures*, *194*, 468–477. https://doi.org/10.1016/j.compstruct.2018.03.070

[24] Thomas, B. S., Gupta, R. C., & Panicker, V. J. (2016). Recycling of waste tire rubber as aggregate in concrete: durability-related performance. *Journal of Cleaner Production*, *112*, 504–513. https://doi.org/10.1016/j.jclepro.2015.08.046

[25] Thomas, B. S., & Gupta, R. C. (2016). A comprehensive review on the applications of waste tire rubber in cement concrete. *Renewable and Sustainable Energy Reviews*, *54*, 1323–1333. https://doi.org/10.1016/j.rser.2015.10.092

[26] Shu, X., & Huang, B. (2014). Recycling of waste tire rubber in asphalt and portland cement concrete: An overview. *Construction and Building Materials*, *67*, 217–224. https://doi.org/10.1016/j.conbuildmat.2013.11.027

[27] Na, O., & Xi, Y. (2016). Mechanical and durability properties of insulation mortar with rubber powder from waste tires. *Journal of Material Cycles and Waste Management*, *19*(2), 763–773. https://doi.org/10.1007/s10163-016-0475-2